J Nanostruct 13(1): 37-47, Winter 2023

RESEARCH PAPER

Evaluation of the Performance of an Activated Sludge Bioreactor for the Sulfide Removal in the Presence of Nanoparticles: Kinetic Study and Respirometry Test

Jafar Abdi [1], *Seyyed Hamid Esmaeili-Faraj* [1]*, *Mohsen Nasr Esfahany* [2]

[1] *Faculty of Chemical and Materials Engineering, Shahrood University of Technology, Shahrood, Iran*

[2] *Department of Chemical Engineering, Isfahan University of Technology, Isfahan, Iran*

ARTICLE INFO

Article History:
Received 11 October 2022
Accepted 27 December 2022
Published 01 January 2023

Keywords:
Activated sludge bioreactor
Bio-kinetic parameters
Nanoparticles
Respirometry test
Sulfide removal

ABSTRACT

In this project, experimental investigations were performed to measure the bio-kinetic parameters of the sulfide removal using an activated sludge bioreactor (ASBR) in the presence of nanoparticles. For this aim, silica nanoparticles (NPs) and exfoliated graphene oxide (GO) nanosheets were synthesized and characterized using FTIR, XRD, and TEM analysis. Then, three types of bioreactor systems, including activated sludge without nanoparticles (AS), in the presence of SiO_2 NPs, and GO nanosheets, were utilized for different ranges of sulfide concentrations. The variation of pH values in the ASBR systems was investigated during the kinetic experiments. Respirometry tests were employed to calculate the maximum yield factor (Y) and endogenous decay coefficient (k_d) in Monod's model and the maximum cell growth rate during the sulfide removal. Moreover, different kinetic models, including Monod, first-order, second-order, Moser, and Contois, were compared. The values of the R^2 coefficient (0.992, 0.927, and 0.976 for AS, SiO_2, and GO bioreactor systems, respectively) showed that the Monod model was appropriately fitted with the experimental data, and the SiO_2 sample had the best condition for both sulfide removal and biomass growth and GO sample had the worst performance.

How to cite this article
Abdi J., Esmaeili-Faraj S H., Nasr Esfahany M. Evaluation of the Performance of an Activated Sludge Bioreactor for the Sulfide Removal in the Presence of Nanoparticles: Kinetic Study and Respirometry Test. J Nanostruct, 2023; 13(1):37-47. DOI: 10.22052/JNS.2023.01.005

INTRODUCTION

Nowadays, the presence of sulfurous compounds in aqueous media has been converted to one of the most serious risks due to their high toxicity. Hydrogen sulfide (H_2S), as a volatile organic compound, is the most common form of sulfurous compounds and exists in both forms of bisulfide (HS^-) and sulfide ions (S^{2-}) in wastewater. Usually, two moles of O_2 are consumed per mole of S^{2-}, and therefore sulfide ions decrease the dissolved oxygen in water [1-5]. Moreover, sulfurous compounds are so toxic and count as a huge threat to the aqueous ecosystem. Thus, it is necessary to choose a suitable, economic, and environmentally friendly technique to eliminate this pollutant from wastewaters and waste gases [4-6]. Different physicochemical methods, including advanced oxidation processes (AOPs) and catalytic conversion, have been employed to remove sulfide ions from wastewaters by the oxidation of sulfide to either sulfate or elemental sulfur [7-9]. Since these methods operate with

* *Corresponding Author Email: h.esmaeili@shahroodut.ac.ir*

considerable energy consumption and need some chemicals, more cost-effective approaches are required. Nowadays, physicochemical processes, such as oxidation and direct air stripping, are commonly used for sulfide removal [10-13]. Nonetheless, biological methods have attracted great attention due to their more practical and economic features comparison to physicochemical methods under the same operational conditions [4]. It is well-known that the activated sludge process is the most commonly utilized technique for biological wastewater treatment [9].

Substrate removal occurs along with the growth of biomass during the biodegradation process. The rate of this process can be affected by various parameters involving microbial population, the chemical structure of the substrate, pH, oxygen concentration, temperature, and accessibility of nutrients [6, 14]. Also, the adsorption of pollutants directly relates to biomass concentration, and its performance improves with increasing the concentration of biomass in a bioreactor [15]. In addition, the performance of microorganisms has been dramatically affected by the presence of nanoparticles (NPs) by their development in different processes [16, 17]. Recently, various kinds of NPs have been explored in wastewater, which can be adsorbed onto activated sludge (AS) [18, 19]. Consequently, some researches were performed to determine the effect of NPs' existence on biological wastewater treatment methods, especially the AS process. Many studies have been evaluated the toxicity of different NPs, such as SiO_2, TiO_2, Ag, Zn, and Cu nanoparticles on AS [17, 20-24]. Nevertheless, the literature survey showed that despite nanoparticles' application in wastewater treatment [25-27], a few works have been reported the sulfide removal from wastewater using biological systems in the presence of nanoparticles. Rollemberg et al. [28] compared the performance of aerobic granular sludge (AGS) and activated sludge flocs (ASF) for eliminating organic contaminants during nitrification, denitrification, and dephosphatation processes. They found that the AGS system produced less sludge and a higher endogenous consumption rate than ASF, and the yield factors (Y) were obtained 0.36 and 0.55 g VSS/g COD for AGS and ASF, respectively. Akdemir et al. [29] studied the effect of carbon nanotubes (CNTs) on removing heavy metals in a continuous activated sludge process. They found that the presence of CNTs increased the amount of COD and also the removal efficiencies of nickel (79.99%), copper (99%), and chromium (99%). In another work, Akdemir et al. [30] studied the presence of CNTs on the performance of activated sludge treatment. The results indicated that adding CNTs from 10 to 30 mg/L led to enhancing nitrogen removal from 65% to 75% and decreasing ammonium concentration to 70%. Adding CNTs increased the saturation constant (K_s) from 1406 to 2355 mg/L, while the Y factor remained without significant change. Alizad Oghyanous et al. [31] employed four different submerged membrane bioreactors in a lab-scale to determine biokinetic coefficients and optimize their performance during eight months. The results revealed that yield factor, maximum growth rate (μ_{max}), the half-velocity coefficient for the substrate (K_s), and endogenous decay coefficient (K_d) were achieved between 0.0733-0.310 mg/mg, 1.249-3.672 day^{-1}, 1-3.156 mg/L, and 0.985-3.119 day^{-1}, respectively. Moreover, the best operating condition for activated sludge was obtained at 15 days sludge residence time and COD loading of 0.1 (g COD/L. day).

The daily development of nanoparticles in the different processes has caused remarkable effects on the performance of microorganisms. On the other hand, studying and evaluating the biological removal of sulfide pollutants by comprehensive comparison between the kinetic models of specific growth of biomass in different bioreactors can help the improvement of their performance. Therefore, the object of the present work is to investigate the effect of GO nanosheets and SiO_2 nanoparticles on the reaction kinetic of the sulfide removal in the activated sludge bioreactor (ASBR) system using a respirometry test. The remaining sections of this study are outlined as follows: First, the GO and SiO_2 nanomaterials are synthesized and then analyzed to investigate the physical and chemical characteristics. Then, the activated sludge system is employed to remove sulfide ions in the presence of the nanomaterials. Next, the bio-kinetic parameters are determined using a respirometry test, and different kinetic models are also compared. The paper ends with a conclusion, which recaps the main results of the investigation.

MATERIAL AND METHODS

Materials

Graphite powder (99.99 % purity), nitric acid (HNO_3), sulfuric acid (H_2SO_4), hydrochloric

acid (HCl), and potassium chlorate ($KClO_3$) were purchased from Merck Company. Ammonia solution (25%), tetraethyl orthosilicate (TEOS), and ethanol were obtained to prepare silica nanoparticles from Merck Company. Sodium sulfide hydrate ($Na_2S.9H_2O$, 60% purity) was obtained as a substrate from Samchun Pure Chemical Company (SPCC). Sulfide ion concentration was measured using iodine, potassium bi-iodate (HI_2KO_6), sodium thiosulfate ($Na_2S_2O_3$), and potassium iodide (KI) purchased from Merck Company.

Characteristics instruments

Fourier transform infrared spectroscopy (FT-IR) (Lambda-25, PerkinElmer, USA) was employed to determine the functional groups that exist on the surface of prepared materials. X-ray diffraction (XRD) (PW3710; Philips, Netherlands) was utilized to indicate the crystallinity of the prepared nanomaterials. The size and surface morphology of the exfoliated graphene oxide and silica nanoparticles were characterized by transmittance electron microscopy (TEM) (PHILIPS CM120, USA). DO-meter (DO-5510 Lutron Electronic Enterprise Company, Taiwan) was operated to measure dissolved oxygen concentration.

Synthesis of nanomaterials

According to the literature [12, 32], the exfoliated graphene oxide (GO) nanosheets were prepared from graphite powder using the Hummer's method. The summary of the synthesis procedure is shown in Fig. 1a. The amorphous silica (SS) nanoparticles as also synthesized in a simple way. As shown in Fig. 1b, firstly, 1 mol TEOS was dissolved in 6.3 mol ethanol. Then a mixture containing 1.8 mol aqueous ammonia (25%) and 6.3 mol ethanol was added to the previous solution and stirred for an hour. Eventually, the mixture was washed several times with distilled water and dried 24 h at 60 °C to obtain SiO_2 nanoparticles as powders.

Measurement of biomass growth and sulfide removal

The mixture liquor volatile suspended solid (MLVSS) was measured to determine the biomass growth based on a standard method reported in

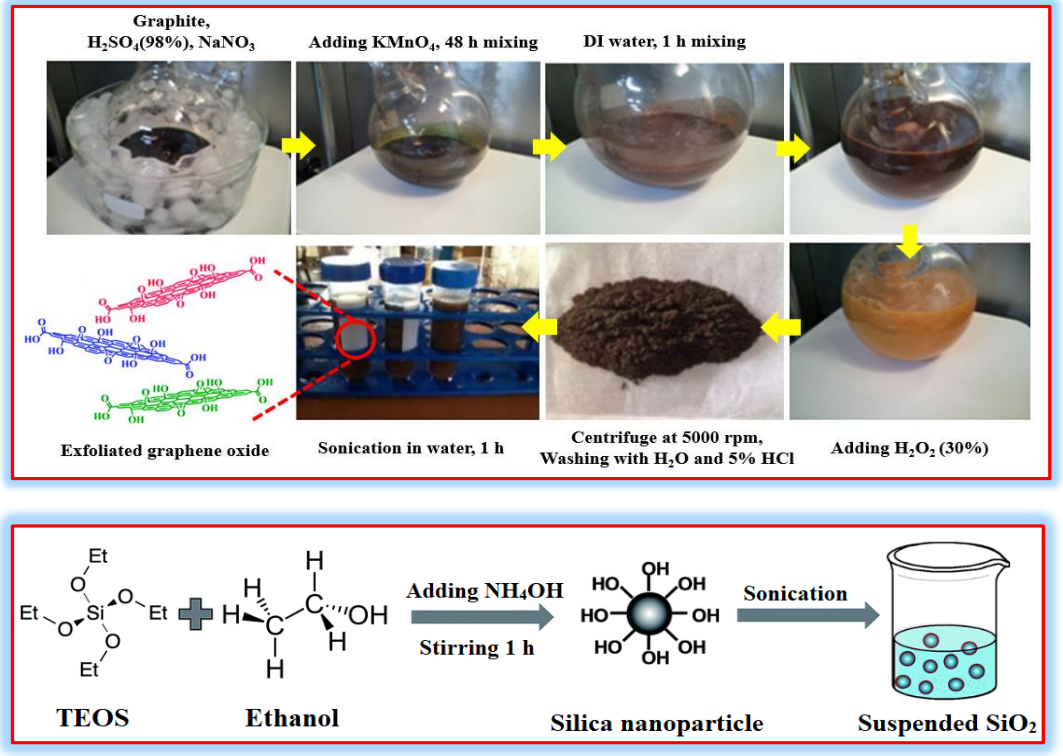

Fig. 1. The synthesis procedure of the exfoliated GO nanosheets and SiO_2 nanoparticles.

the literature (2540 Solids#43) [33]. Sulfide ion concentration was also measured through the iodometric method [33].

Determination of bio-kinetic parameters

A respirometry test was used to obtain bio-kinetic parameters in the first step. It is based on mass balance as the following [34]:

$$(-\Delta S) + (-\Delta O) = \Delta X \quad (1)$$

Where ΔX is the generated biomass, Δ0 is the consumed oxygen, and (-ΔS) is the total consumed substrate. Eq. (1) can be written as the following:

$$\frac{\mathrm{d}O_2}{\mathrm{dt}} = -\frac{\mathrm{d}S}{\mathrm{dt}} - \frac{\mathrm{d}X}{\mathrm{dt}} \quad (2)$$

The amount of produced biomass per unit of the consumed substrate is called the yield factor (Y):

$$Y = \frac{\Delta \mathrm{X}}{-\Delta \mathrm{S}} \quad (3)$$

Monod's growth model is used to define two terms on the right-hand side of Eq. (2) as [35]:

$$-\frac{\mathrm{d}S}{\mathrm{d}t} = \frac{\mu_{max}}{Y}\frac{S}{K_s + S}X \quad (4)$$

$$\frac{\mathrm{d}X}{\mathrm{dt}} = \mu_{max}\frac{S}{K_s + S}X - k_d X \quad (5)$$

where μ_{max}, K_S and k_d are attributed to the maximum growth rate (day^{-1}), the half-velocity coefficient for the substrate (gS/L) and endogenous decay coefficient (day^{-1}), respectively.

Oxygen uptake rate (OUR) is an important parameter obtained by a respirometry test. Eq. (6) is obtained by substituting Eqs. (4) and (5) into Eq. (2):

$$OUR = \frac{\mathrm{d}O_2}{\mathrm{dt}} = \left[\left(\frac{1-Y}{Y}\right)\frac{\mu_{max}S}{K_S + S} + k_d\right].X \quad (6)$$

In Eq. (6), the first term is the exogenous respiration related to substrate consumption [36]. The second term on the right-hand side is called endogenous respiration, which defines the oxygen consumption of bacteria for the hydrolyzation of dead cells, their movement, and cellular proliferation.

The bio-kinetic parameters (k_d and *Y*) can be obtained by measuring the oxygen consumption rate. These two parameters demonstrate the interaction between the biomass and the substrate. The endogenous contribution can be determined by operating a bioreactor without any substrate (fixing S=0). Therefore, Eq. (6) is transformed to the following equation through this assumption [36].

$$\frac{OUR}{X} = k_d \quad (7)$$

Fig. 2 schematically depicts the details of a respirometry reactor. A respirometry test was performed two weeks after starting the biodegradation process to remove sulfide ions. A specific volume of mixed liquor (500 mL) from each bioreactor was transferred to the respirometry reactor. The variation of dissolved oxygen (DO) concentration in mixed liquor is approximately linear, and its slope equals OUR. Primarily, the concentration of DO in the mixed liquor was measured without any substrate feeding. Then, the endogenous decay coefficient (k_d) was calculated by Eq. (7). In the next step, sulfide ion was added to the respirometry reactor, and the concentration of substrate reached the finite level of 8000 mg/L. After that, aeration was started and continued for 5 min and DO concentration was frequently measured. To overcome oxygen limitation, fresh air was supplied so that DO concentration was maintained at greater than 2 mg/L during reactor operation [6]. To assess the influence of nanoparticles, the same procedure was carried out in the presence of silica and GO samples.

In the second step, the variations of substrate concentration over time were measured using the iodometric method to obtain μ_{max} and K_S. In this step, the sulfide ion was added to bioreactors with the initial concentration of 2500 mg/L. Biomass growth was calculated as the difference of MLVSS at the beginning and end of the test.

For the calculation of μ_{max} and K_S, Monod's model is rearranged as below [36]:

$$\frac{\ln\left(\frac{S_0}{S}\right)}{S_0 - S} = -\frac{1}{K_S} + \frac{k}{K_S}\frac{t\bar{X}}{S_0 - S} \quad (8)$$

where *k* is the ratio of μ_{max} to *Y*, $\bar{X}$ is the average biomass concentration during the process, and S_0 is the initial sulfide ion concentration.

RESULTS AND DISCUSSION

Characterization of the prepared nano-materials

To determine the functional groups and the

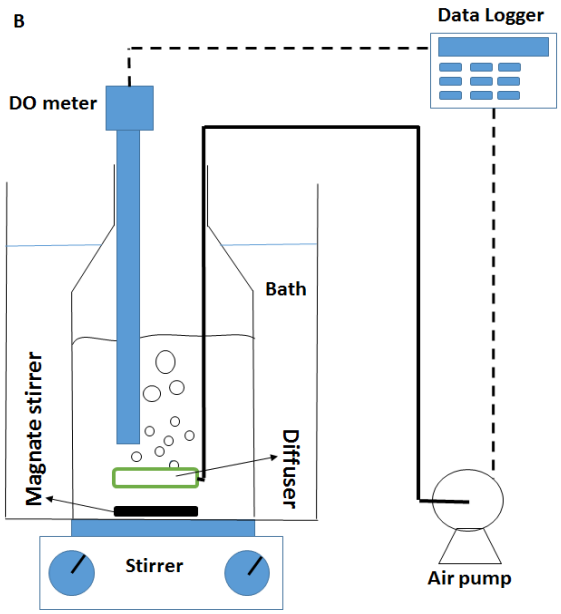

Fig. 2. Schematic of the bioreactor for respirometry test.

surface characteristics of the GO nanosheets and silica nanoparticles, the FTIR spectra were studied in the range of 4000–500 cm^{-1}. As shown in Fig. 3, the spectrum of the GO nanosheets illustrates the major stretching vibrations at 3460, 1728, 1622, 1167, and 1051 cm^{-1}, which belong to OH, -C=O, C=C, C-O, and C-O-C groups, respectively [37]. Siloxane group (Si-O-Si) and silanol group (Si-O-H) bonds can be detected from the FTIR spectra of the silica nanoparticle [8]. Fig. 4 represents XRD patterns of the GO nanosheets and silica nanoparticles. A broad apparent peak at 2θ = 24° belongs to the amorphous structure of the SiO_2 nanoparticles [38]. For the case of the GO, some peaks are specifically observed at 2θ = 10.1°, 24.7°, and 26.5° which correspond to the (002) crystal plane of the graphene oxide, reduced graphene oxide, and graphite, respectively [37, 39]. Moreover, the TEM images of the GO and SiO_2 nanomaterials are shown in Fig. 4. As can be seen, the thickness of the GO nanosheets is less than 20 nm, and they have an exfoliated structure. Silica nanoparticles show spherical morphology with nano-size below 5 nm.

Determination of bio-kinetic parameters

The results of the dissolved oxygen measurement for three bioreactors of AS, SS, and GO are presented in Figs. 5a, b, and c, respectively. During the respirometry test, an initial measurement was performed in the endogenous step, and then the substrate was added followed by aeration three times. Indeed, OUR can be determined by the slope of the fitted line on the variations of DO concentration with time. Table 1 summarizes the obtained results from the respirometry test. Accordingly, the SS sample has the maximum yield factor, which depicts the amount of biomass generation per unit of substrate consumption. It shows that bacteria growth is enhanced in the presence of SS nanoparticles. Also, the GO nanosheet has the minimum yield factor related to its antibacterial activity. Furthermore, Table 1 represents the endogenous decay coefficient values, (k_d) which are very low in comparison with the exogenous term (first term in the right) in Eq. (6). Therefore, we can ignore the endogenous activity term.

To determine the other bio-kinetic parameters, a respirometry test cannot be helpful. Therefore, other methods should be investigated to obtain these parameters. According to Eq. (8), the changes of substrate concentration are recorded during the time, and then values of $[\ln(S_0/S)/(S_0-S)]$ versus $[t\bar{X}/(S_0-S)]$ for each bioreactor are separately drawn. Then, a straight line is obtained by fitting on the experimental data. The slope of this line is k/K_s, and its intercept is $-1/K_s$. The

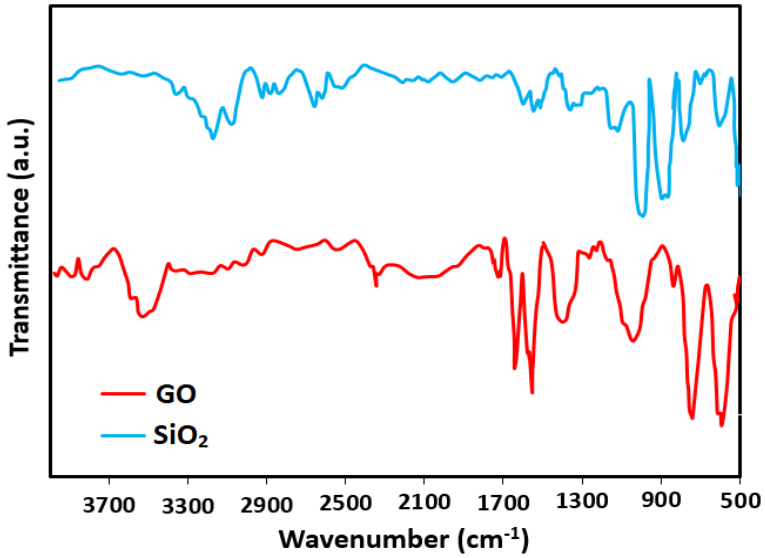

Fig. 3. FT-IR spectra of the synthesized graphene oxide nanosheets and SiO_2 nanoparticles.

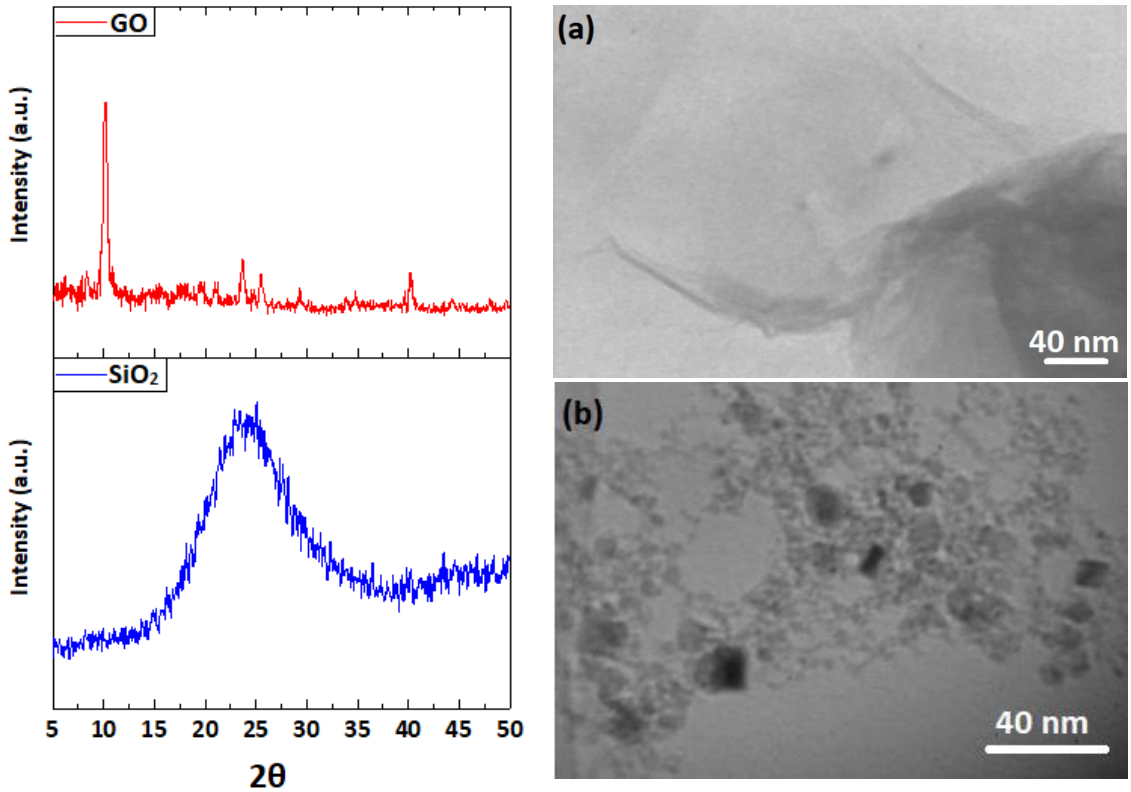

Fig. 4. XRD patterns of the prepared materials (left side) and TEM images of: a) Graphene oxide nanosheets and b) SiO_2 nanoparticles (right side).

summary of the calculations is presented in Table 2. Comparing different kinetic models, such as Monod, first-order, second-order, Moser, and Contois, in terms of R^2 values show that Monod's

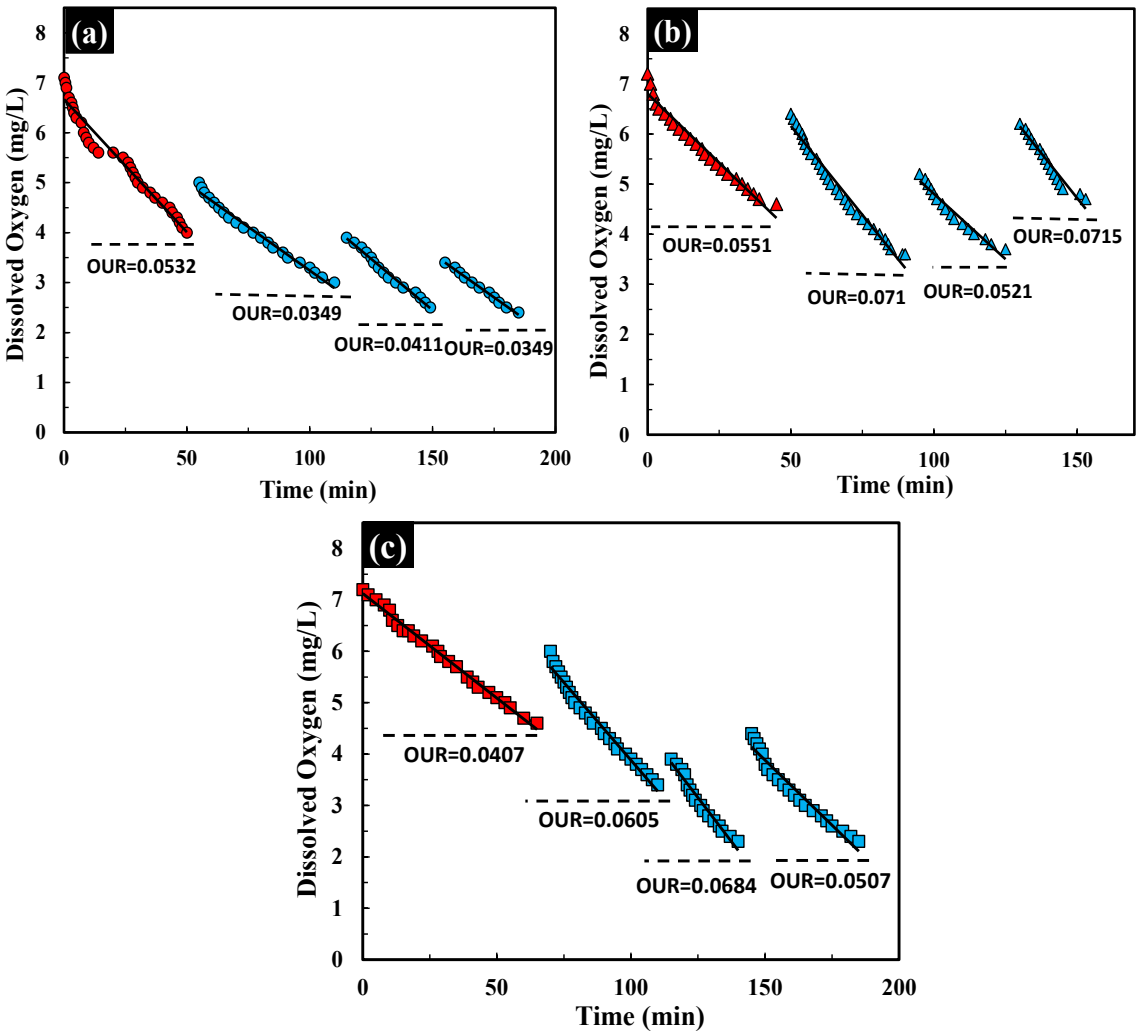

Fig. 5. Dissolved oxygen measurement in respirometry test for three bioreactors: (a) activated sludge (AS) with S_0=8989 mg/L and X_0=9530 mg/L, (b) SiO_2 nanoparticles (SS) with S_0=8731 mg/L and X_0=10990 mg/L, and (c) graphene oxide nanosheets (GO) with S_0=8405 mg/L and X_0=10340 mg/L. (For all cases T=25 ˚C & pH=8).

Table 1. Results of the respirometry test for different bioreactor systems.

Sample	OUR	$OUR_{avg.}$ (mg/L. min)	Biomass (mg/L)		Substrate (mg/L)		k_d (day^{-1})	Yield
			Initial	Final	Initial	Final		
AS	0.0532	0.0370	9530	10105	8989.0	6572.1	0.00780	0.2379
SiO_2	0.0555	0.0649	10990	11575	8731.1	6531.3	0.00708	0.2659
GO	0.0407	0.0599	10340	10775	8405.2	6232.6	0.00555	0.2002

model is appropriately fitted with the experimental data for AS, SiO_2, and GO ASBRs better than the others. The maximum cell growth rate, μ_{max}, is a factor that characterizes the high variation of biomass weight per time and corresponds to the exponential stage in the bacteria growth curve. Larger values of μ_{max} show that the biomass production is increased. As shown in Fig. 6, the maximum specific growth rates of SiO_2, AS, and GO bioreactor systems are μ_{max} =0.1871, 0.1667,

Table 2. Obtained results of the bio-kinetic parameters for different models.

Model	Linearized form	Sample	K_s (mg/L)	k (day^{-1})	μ_{max} (day^{-1})	n	R^2
First order	$ln\frac{S_0}{S} = k_1\bar{X}t$	AS	55.11	1.17	-	-	0.783
		SiO_2	78.19	2.12	-	-	0.687
		GO	65.12	1.12	-	-	0.690
Second order	$\frac{1}{S}-\frac{1}{S_0} = k_2\bar{X}t$	AS	44.30	2.98	-	-	0.457
		SiO_2	63.02	3.41	-	-	0.769
		GO	57.90	2.21	-	-	0.703
Monod	$\frac{\ln\left(\frac{S_0}{S}\right)}{S_0-S} = -\frac{1}{K_s}+\frac{k}{K_s}\frac{t\bar{X}}{S_0-S}$	AS	28.01	3.92	0.1778	-	0.992
		SiO_2	29.07	4.30	0.1701	-	0.927
		GO	29.85	3.72	0.1335	-	0.976
Moser	$\frac{(S^{1-n}-S_0^{1-n})}{S_0-S} = -\frac{1}{K_s(1-n)}+\frac{k\bar{X}t}{K_s(1-n)(S_0-S)}$	AS	37.40	3.21	0.2586	2.86	0.569
		SiO_2	44.12	4.45	0.2103	2.22	0.775
		GO	64.14	2.51	0.1660	2.09	0.680
Contois	$\frac{\ln\left(\frac{S_0}{S}\right)}{S_0-S} = -\frac{1}{K_S\bar{X}}+\frac{k}{K_S}\frac{t}{S_0-S}$	AS	34.56	4.01	0.9325	-	0.698
		SiO_2	51.18	5.11	1.1434	-	0.551
		GO	33.19	3.98	0.7447	-	0.622

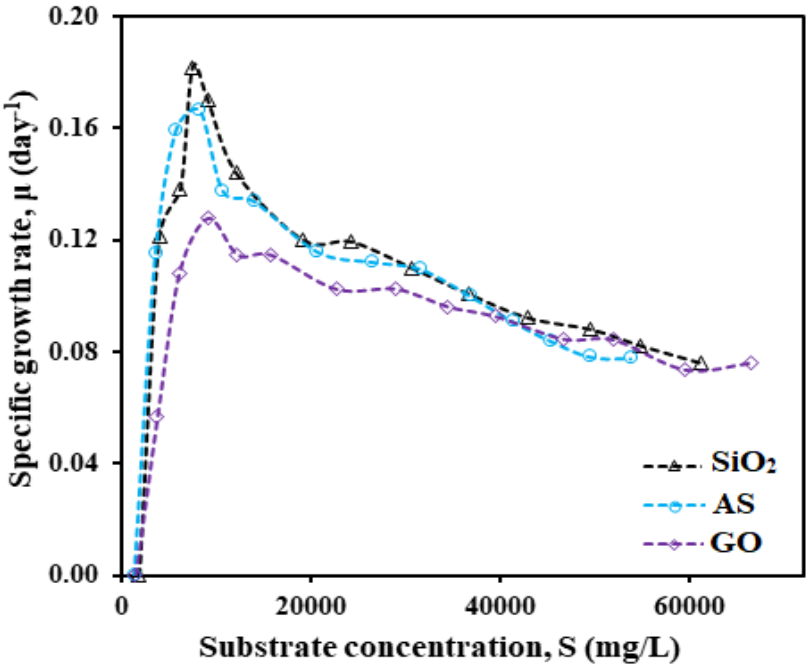

Fig. 6. The effect of sulfide concentration on the specific growth rate of biomass in different ASBR systems. (For all cases T=25 ˚C & pH=8).

and 0.1277 day^{-1}, respectively. The maximum cell growth rate of the silica sample reaches the highest value comparison to the other samples. On the other side, GO presents a minimum value. This result is consistent with data of yield in respirometry results. The half-velocity coefficient,

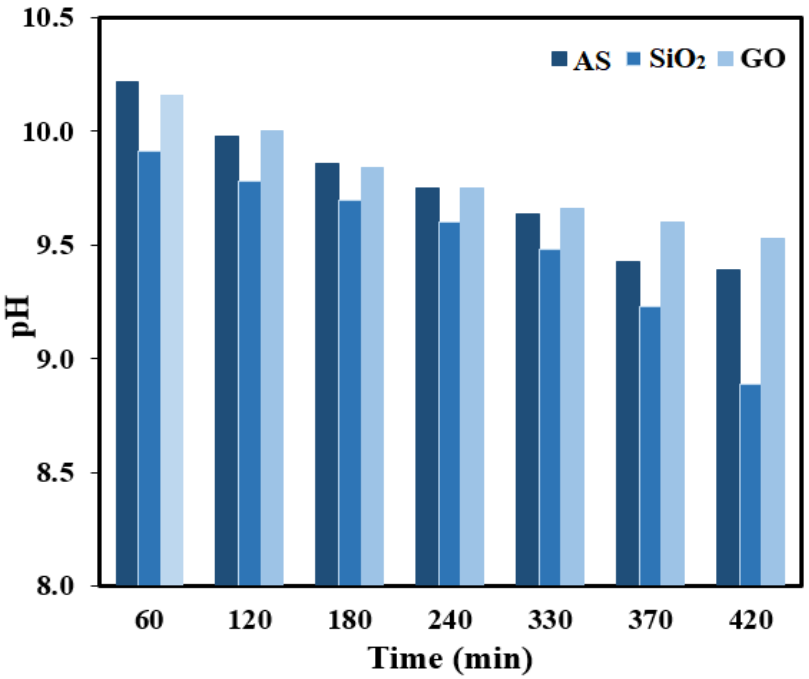

Fig. 7. Measured pH values of bioreactors during sulfide removal in a bioreactor. AS with S_0=2077 mg/L and X_{avg}=7217 mg/L, SS with S_0=2417 mg/L and X_{avg}=7757 mg/L, GO with S_0=2580 mg/L and X_{avg}=7440 mg/L. (For all cases T=25 ˚C).

K_S, is a constant value for each substrate and shows whether the substrate is appropriate for the degradation in the special bioreactor or not. Smaller values of K_S are desirable. Table 2 shows that there is not a remarkable difference between values of K_S for various bioreactors because the substrate and bacteria are similar in all samples.

The pH value of bioreactors is accounted as one of the most critical factors which affect microbial growth. The structure and activity of proteins depend on the solution pH. So, it can be expected that the pH of media affects the material transfer process to the reactions and consequently the kinetic rate of cells. Fig. 7 illustrates the measured pH values in the bioreactor during the kinetic experiments. As can be seen, the pH values are high at the beginning of the reaction, and it decreases with the passage of time. This variation can be attributed to the addition of sodium sulfide, which enhances the pH. Then the solution pH diminishes by the removal of sulfide ions and its conversion to elemental sulfur.

CONCLUSION

In summary, silica nanoparticles and exfoliated graphene oxide were synthesized and employed for sulfide removal in different activated sludge bioreactor systems. Various bio-kinetic parameters, such as yield factor (Y), maximum specific growth rate (μ_{max}), endogenous decay coefficient (k_d), and the half-velocity constant (K_S), were obtained using respirometry experiments for three AS, SiO_2, and GO bioreactor systems. The respirometry test represented the endogenous decay coefficient (k_d) values of 0.00780, 0.00708, and 0.00555 for AS, SiO_2, and GO ASBR system, respectively, which could be ignored in comparison with the exogenous term. The maximum specific growth rates of SiO_2, AS, and GO bioreactor systems were obtained μ_{max}=0.1871, 0.1667, and 0.1277 day^{-1}, respectively. These results demonstrated that biomass growth and sulfide removal in the SiO_2 sample was better than the others, and GO had the worst performance. Investigating different kinetic models showed that the experimental data were in good accordance with Monod's model. Development and kinetic study can be advantageous and efficient due to their analyzability and investigation of different operational parameters in the biological process

of pollutants removal.

ACKNOWLEDGMENTS

The present work was accomplished in faculty of chemical and materials engineering, Shahrood University of Technology.

CONFLICT OF INTEREST

The authors declare that there is no conflict of interests regarding the publication of this manuscript.

REFERENCES

1. Vaiopoulou E, Melidis P, Aivasidis A. Sulfide removal in wastewater from petrochemical industries by autotrophic denitrification. Water Res. 2005;39(17):4101-4109.
2. Hassanvand A, Esmaeili-Faraj SH, Moghaddam MS, Moradi R. Characterization of a New Structured Packing by Computational Fluid Dynamics. Chemical Engineering & Technology. 2020;44(1):156-163.
3. Esmaeili-Faraj SH, Hassanzadeh A, Shakeriankhoo F, Hosseini S, Vaferi B. Diesel fuel desulfurization by alumina/polymer nanocomposite membrane: Experimental analysis and modeling by the response surface methodology. Chemical Engineering and Processing - Process Intensification. 2021;164:108396.
4. Altaş L, Büyükgüngör H. Sulfide removal in petroleum refinery wastewater by chemical precipitation. J Hazard Mater. 2008;153(1-2):462-469.
5. Zaker S, Sharafi A, Parvizi R, Esmaeili-Faraj SH, Ghaseminejad E. Swelling behavior of heavy crude oil in carbonated water at the presence of Na_2SO_4 and Mg_2SO_4. Journal of Petroleum Exploration and Production Technology. 2020;10(7):2759-2769.
6. Biotechnology for Odor and Air Pollution Control. Springer Berlin Heidelberg; 2005.
7. Chen C, Wang A, Ren N, Lee D, Lai J. High-rate denitrifying sulfide removal process in expanded granular sludge bed reactor. Bioresour Technol. 2009;100(7):2316-2319.
8. Esmaeili-Faraj SH, Nasr Esfahany M. Absorption of Hydrogen Sulfide and Carbon Dioxide in Water Based Nanofluids. Industrial & Engineering Chemistry Research. 2016;55(16):4682-4690.
9. Esmaeili-Faraj SH, Esfahany MN, Darvanjooghi MHK. Application of water based nanofluids in bioscrubber for improvement of biogas sweetening in a pilot scale. Chemical Engineering and Processing - Process Intensification. 2019;143:107603.
10. Janssen AJH, Lettinga G, de Keizer A. Removal of hydrogen sulphide from wastewater and waste gases by biological conversion to elemental sulphur. Colloids Surf Physicochem Eng Aspects. 1999;151(1-2):389-397.
11. Lyn TL, Taylor JS. Assessing Sulfur Turbidity Formation Following Chlorination of Hydrogen Sulfide in Groundwater. Journal - American Water Works Association. 1992;84(9):103-112.
12. Moghadam G, Abdi J, Banisharif F, Khataee A, Kosari M. Nanoarchitecturing hybridized metal-organic framework/graphene nanosheet for removal of an organic pollutant. J Mol Liq. 2021;341:117323.
13. Abdi J, Hadipoor M, Hadavimoghaddam F, Hemmati-Sarapardeh A. Estimation of tetracycline antibiotic photodegradation from wastewater by heterogeneous metal-organic frameworks photocatalysts. Chemosphere. 2022;287:132135.
14. Esmaeili Faraj SH, Esfahany MN, Kadivar M, Zilouei H. Vinyl chloride removal from an air stream by biotrickling filter. Journal of Environmental Science and Health, Part A. 2012;47(14):2263-2269.
15. Singh A., Shareefdeen Z. Biotechnology for odor and air pollution control. 2005: Berlin: Springer-Verlag.
16. Esmaeili-Faraj, S.H. and M. Nasr Esfahany, Influence of SiO2 and graphene oxide nanoparticles on efficiency of biological removal process. Environ Technol, 2017. 38(21): p. 2763-2774.
17. Choi O, Hu Z. Size Dependent and Reactive Oxygen Species Related Nanosilver Toxicity to Nitrifying Bacteria. Environmental Science & Technology. 2008;42(12):4583-4588.
18. Kiser MA, Ryu H, Jang H, Hristovski K, Westerhoff P. Biosorption of nanoparticles to heterotrophic wastewater biomass. Water Res. 2010;44(14):4105-4114.
19. Limbach LK, Bereiter R, Müller E, Krebs R, Gälli R, Stark WJ. Removal of Oxide Nanoparticles in a Model Wastewater Treatment Plant: Influence of Agglomeration and Surfactants on Clearing Efficiency. Environmental Science & Technology. 2008;42(15):5828-5833.
20. Zheng X, Wu R, Chen Y. Effects of ZnO Nanoparticles on Wastewater Biological Nitrogen and Phosphorus Removal. Environmental Science & Technology. 2011;45(7):2826-2832.
21. Kocbek P, Teskač K, Kreft ME, Kristl J. Toxicological Aspects of Long-Term Treatment of Keratinocytes with ZnO and TiO_2 Nanoparticles. Small. 2010;6(17):1908-1917.
22. Ganesh R, Smeraldi J, Hosseini T, Khatib L, Olson BH, Rosso D. Evaluation of Nanocopper Removal and Toxicity in Municipal Wastewaters. Environmental Science & Technology. 2010;44(20):7808-7813.
23. Abdi J. Synthesis of Ag-doped ZIF-8 photocatalyst with excellent performance for dye degradation and antibacterial activity. Colloids Surf Physicochem Eng Aspects. 2020;604:125330.
24. Mn-Etched Zeolitic Imidazolate Framework-67 Nanostructures for Biomimetic Superoxide Anion Sensing. American Chemical Society (ACS).
25. Yousefi SR, Sobhani A, Alshamsi HA, Salavati-Niasari M. Green sonochemical synthesis of $BaDy_2NiO_5/DyO_3$ and $BaDy_2NiO_5/Ni_O$ nanocomposites in the presence of core almond as a capping agent and their application as photocatalysts for the removal of organic dyes in water. RSC Advances. 2021;11(19):11500-11512.
26. Yousefi SR, Amiri O, Salavati-Niasari M. Control sonochemical parameter to prepare pure $Zn_{0.35}Fe_{2.65}O_4$ nanostructures and study their photocatalytic activity. Ultrason Sonochem. 2019;58:104619.
27. Yousefi SR, Alshamsi HA, Amiri O, Salavati-Niasari M. Synthesis, characterization and application of Co/Co_3O_4 nanocomposites as an effective photocatalyst for discoloration of organic dye contaminants in wastewater and antibacterial properties. J Mol Liq. 2021;337:116405.
28. Rollemberg SLdS, Barros ANd, Lira VNSA, Firmino PIM, dos Santos AB. Comparison of the dynamics, biokinetics and microbial diversity between activated sludge

flocs and aerobic granular sludge. Bioresour Technol. 2019;294:122106.
29. Akdemir ÜÖ. Removal of heavy metals from mixed domestic and industrial wastewater by activated sludge process using MWCNT. International Journal of Global Warming. 2020;22(3):315.
30. Akdemir ÜÖ. Determination of the effect of multi-walled carbon nanotube on the treatment efficiency and design parameters in the activated sludge systems. DESALINATION AND WATER TREATMENT. 2020;192:166-175.
31. Alizad Oghyanous F, Etemadi H, Yegani R. Foaming control and determination of biokinetic coefficients in membrane bioreactor system under various organic loading rate and sludge retention time. Biochem Eng J. 2020;157:107491.
32. Esmaeili Faraj SH, Nasr Esfahany M, Jafari-Asl M, Etesami N. Hydrogen Sulfide Bubble Absorption Enhancement in Water-Based Nanofluids. Industrial & Engineering Chemistry Research. 2014;53(43):16851-16858.
33. Simmons GM. Standard Methods for the Examination of Water and Waste Water. A. E. Greenberg , L. S. Clesceri , A. D. Eaton. J N Am Benthol Soc. 1993;12(3):308-309.
34. Ordaz A, López JC, Figueroa-González I, Muñoz R, Quijano G. Assessment of methane biodegradation kinetics in two-phase partitioning bioreactors by pulse respirometry. Water Res. 2014;67:46-54.
35. Monod J. THE GROWTH OF BACTERIAL CULTURES. Annu Rev Microbiol. 1949;3(1):371-394.
36. Muloiwa M, Nyende-Byakika S, Dinka M. Comparison of unstructured kinetic bacterial growth models. South African Journal of Chemical Engineering. 2020;33:141-150.
37. Abdi J, Vossoughi M, Mahmoodi NM, Alemzadeh I. Synthesis of metal-organic framework hybrid nanocomposites based on GO and CNT with high adsorption capacity for dye removal. Chem Eng J. 2017;326:1145-1158.
38. Kumar Yadav V, Fulekar MH. Green synthesis and characterization of amorphous silica nanoparticles from fly ash. Materials Today: Proceedings. 2019;18:4351-4359.
39. Johra FT, Lee J-W, Jung W-G. Facile and safe graphene preparation on solution based platform. Journal of Industrial and Engineering Chemistry. 2014;20(5):2883-2887.